Detection of cavitation erosion in centrifugal pumps

W. K. Chan
School of Mechanics and Production, Nanyang Technological Institute,
Singapore 9127, Republic of Singapore

This paper presents a method in which the minimum NPSH that a centrifugal pump can operate without risks of erosion can be deduced. It has been recognized that cavitation erosion can only be induced when vapor bubbles collapse near the boundary concerned. Presented in this paper are the results of experiments carried out on a centrifugal impeller in a closed circuit, which show that below the critical NPSH the erosion rate first increases, then decreases, and finally increases for a decreasing NPSH.

Keywords: cavitation; erosion; centrifugal pump

Introduction

That the mere existence of cavitation does not imply that erosion will surely occur has been long recognized by hydraulic designers and engineers. But the detection of when erosion commences has until now been elusive and unpredictable. This can be attributed to the complexities of the flow conditions and to our inability to analyze or model such conditions in a controllable environment.

In industry hydraulic designers guarantee their products up to the 3% head drop, but they too realize that erosive cavitation commences long before the 3% drop in head. To avoid cavitation completely is impractical because severe inlet conditions would be imposed on the operating system and thus reduce the flexibility of the whole system. Industrial experience has shown that pumps operating under incipient cavitation are not subjected to severe erosion that is detrimental to the life of the blades. In the wake of such problems, some hydraulic designers have proposed the idea that the risk of erosion commences as soon as there is a first detachment of vapor bubbles (the NPSH corresponding to this first detachment of vapor bubbles is denoted by f'). Though this will increase the range of pressures that we can operate, it is undeniable that the first detachment of vapor bubbles does not necessarily lead to cavitation erosion. Such vapor bubbles must be brought to collapse close to the moving surfaces to be able to cause erosion.

In view of the above-mentioned problems, experiments at ENSAM have been carried out to determine and to prove the existence of an erosive NPSH (hereby denoted by f_c) below which the risk of erosion commences.

Instrumentation

Experiments are carried out in a closed circuit shown in Figure 1. The impeller has a 249-mm outer diameter and a 213-mm inlet diameter. The diameter of the suction and discharge is 250 mm. A plexiglas tube, as shown in Figure 1, makes visualization and photography of the blades possible. Lighting is provided by a 1540-type stroboscope, and light pulses are tuned in frequency with the impeller's rotational speed. Mercury-water manometers are used to measure the NPSH and the head developed by the impeller. Because as erosion tests on the actual impeller are costly and tedious, we have acquired a microionized lead paint which suitably indicates the eroded surface.

With a mesh tracing method, small finite squares (5 mm by 5 mm) are traced on the suction side of the blades. This enables the eroded surface area to be measured (Figure 2). The location of the zone attacked by cavitation can also be noted with respect to the corresponding form of the cavitation cloud. This method permits direct evaluation of results without dismantling and reassembling the system, which is time consuming and would change the experimental conditions.

Tests are conducted at 1450 r/min and 1150 r/min. Because cavitation forms can only be visualized on the suction side of the impeller, erosion tests on the impeller are carried out for $Q < Q$ adaptation. The flow rates selected are shown in Table 1. The flow rates at 1150 r/min are selected so that they are similar to those at 1450 r/min.

The NPSH of the system is varied from 6 m to 18 m for each flow rate. The blades are observed at 30-min intervals. Direct observation of the eroded surfaces allows the plotting of S (surface area removed in square millimeters) versus time in hours.

For a given flow rate, as the NPSH of the system is decreased, leading edge cavitation commences, followed by developed cavitation and the 3% drop in head. The essence of the method employed is that at f_c the erosion rate (denoted by $\tau = S/T$ mm^2/h) is zero. When the NPSH is decreased below f_c, the erosion rate increases; so by plotting the erosion rate versus NPSH, we will have a curve of the form shown in Figure 3. Intersection of the curve with the horizontal axis gives f_c.

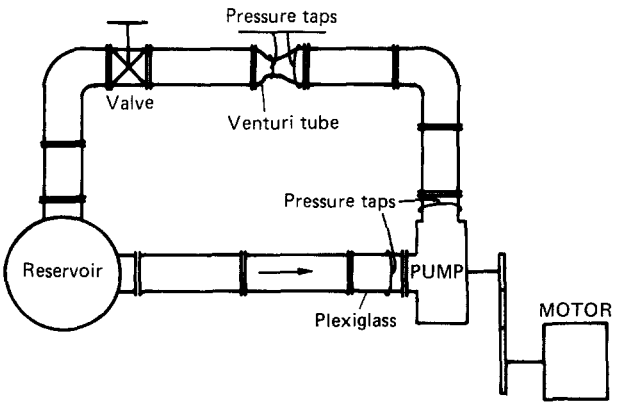

Figure 1 Schematic diagram of experimental layout

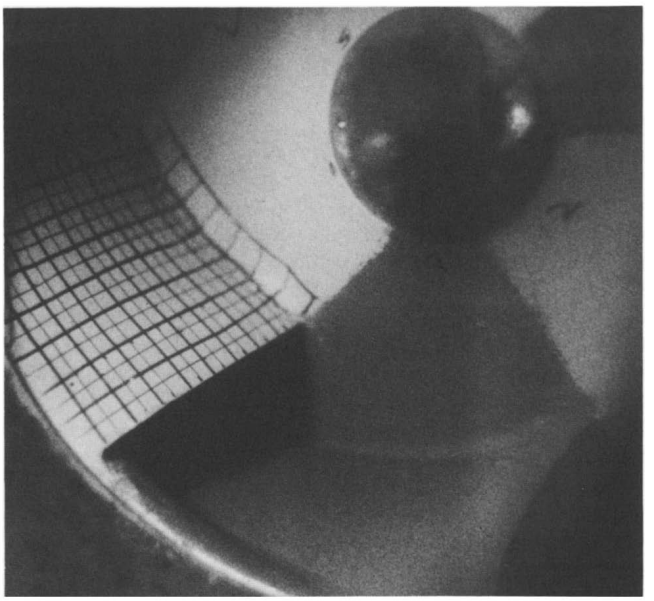

Figure 2 Meshlike configuration traced on blades

Table 1 Choice of speeds and flow rates for experiments

Speed (r/min)	Flow rate (l/s)				
1450	103	118	151	160	172
1150	81	94	120	127	136

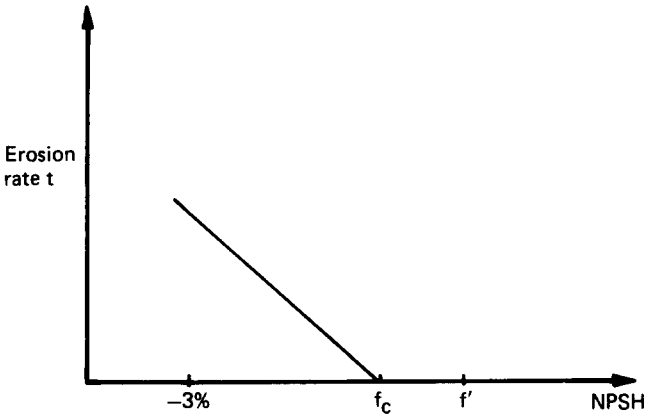

Figure 3 Graph of τ versus NPSH

Discussion

Figures 4 and 5 show the general trend of the variation of the eroded surface with time for an impeller's speed of 1450 r/min and 1150 r/min, respectively.

For $N = 1450$ r/min we observed that for $Q < Q$ recirculation, the curves $S = f(T)$ have a form similar to that of curve a. Direct observation of the eroded zones showed that the flow is unsteady and that "pittings" were distributed throughout the suction side of the blades. For $Q > Q$ recirculation, the curves $S = f(T)$ have a form similar to that of curves b and c. In fact, for curve b, the eroded zone is relatively concentrated, and after a time T_0 the increase in the eroded surface area is insignificant. Hence we can expect the depth of eroded zone to increase. This results from the repeated blows of bubble collapse on the same area. Curve c corresponds to a state of cavitation where only a small surface area is eroded. This can be explained either by the fact that the intensity of the collapse is insufficient to provoke erosion or that the collapse takes place at a distance too far to initiate damage.

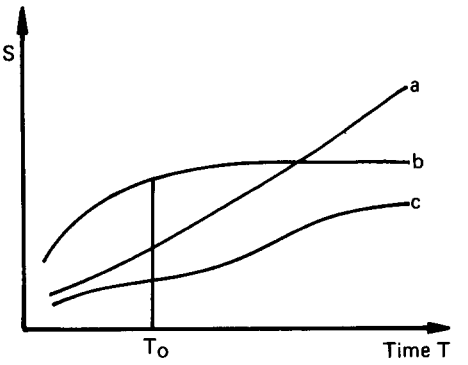

Figure 4 Variation of S with increasing T at 1450 r/min

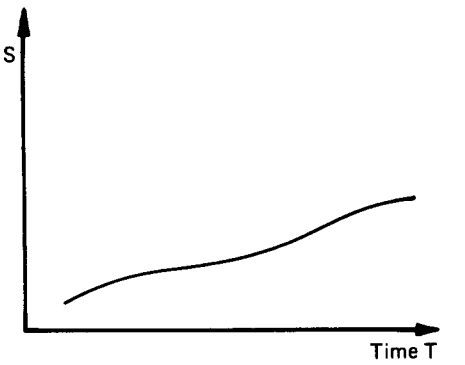

Figure 5 Variation of S with increasing T at 1150 r/min

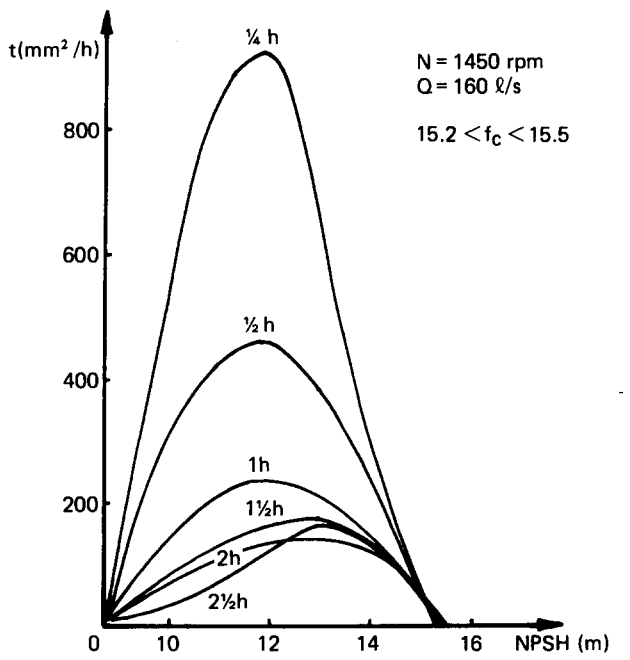

Figure 6 Variation of τ versus NPSH

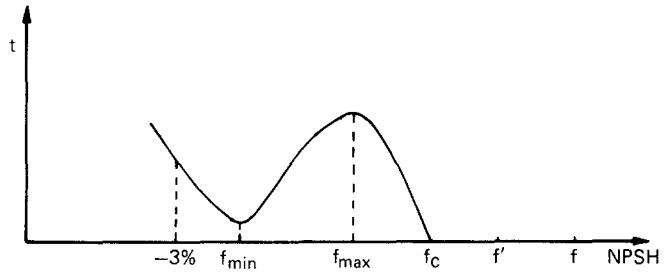

Figure 7 General trend of τ versus NPSH

Table 2 Values of f_c/f' for 1450 and 1150 r/min

N=1450 r/min		N=1150 r/min	
Flow rate (l/s)	$\frac{f_c}{f'}$	Flow rate (l/s)	$\frac{f_c}{f'}$
172	0.75	136	0.91
160	0.72	127	0.96
151	0.83	120	0.91
118	0.81	94	0.75
103	0.49	81	0.55

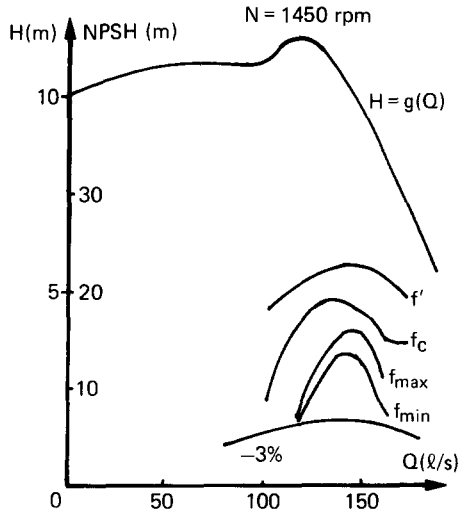

Figure 8 Characteristics of impeller at 1450 r/min

For $N=1150$ r/min the curves $S=f(T)$ indicated in Figure 5 are similar to curve c in Figure 4. The reduction of the eroded surface area can be attributed to the reduction of the impeller's speed. Though the $S=f(T)$ curves have the same form, the experimental results showed that for $Q<Q$ recirculation, the eroded zones are distributed throughout, whereas for $Q>Q$ recirculation the eroded zones are relatively concentrated.

Figure 6 illustrates one of the experimental results where f_c can be deduced for a given flow rate. We also note the existence of a maximum erosion rate and a minimum erosion rate between f_c and NPSH-3%. The NPSHs corresponding to the maximum and minimum erosion rates are denoted by f_{max} and f_{min}, respectively. In general, the variation of τ versus NPSH can be represented in Figure 7. Hence the use of the NPSH-3% as a criterion to avoid erosion is not justifiable, because it lies on the left side of f_{min}. Visual observation of the cavitation state indicates a very developed cavitation sheet at NPSH-3%.

Table 2 tabulates the ratio of f_c to f' for speeds of 1450 r/min and 1150 r/min. In fact, the use of f' as a criterion increases the operating range of the pump as compared to the case where the pump has to operate in the noncavitation state. However, this criterion is subjective because the detection of the first bubble detachment is very difficult by mere observation. Moreover, the first bubble detachment does not necessarily lead to erosion. From our experiments, the criterion f_c is observed to be always smaller than f', so the operating range can be increased. This represents a reduction of operating costs, since the NPSH necessary to avoid the erosion can be reduced.

Figures 8 and 9 illustrate the characteristics of the centrifugal impeller and the various criteria that we have discussed.

A typical cavitation form is shown in Figure 10, where a cloud cavitation is observed near the hub, and a relatively stable sheet cavitation is observed near the shroud.

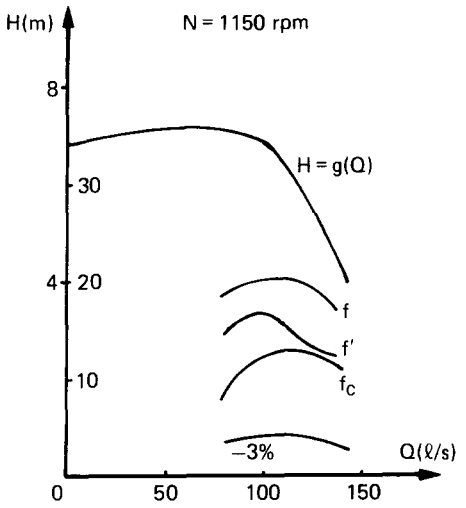

Figure 9 Characteristics of impeller at 1150 r/min

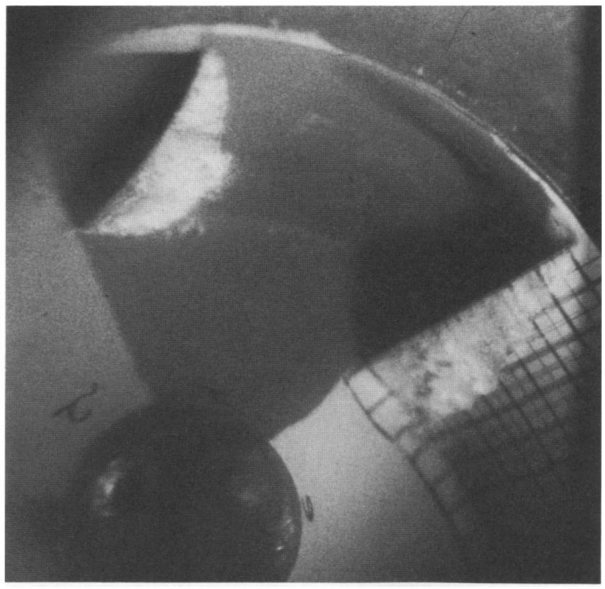

Figure 10 Cavitation form at 1450 r/min, 160 l/s, and NPSH=11.5 m

Conclusion

We have adopted an experimental method in which a new criterion f_c has been determined. This criterion marks the beginning of the risk of erosion that an impeller is subjected to. The use of f_c instead of f' permits a lower NPSH, which is necessary to avoid erosion.

This paper also shows that operation at -3% head is not justifiable since the impeller is in a zone where the cavitation state is extremely developed.

The general trend of τ versus NPSH shows the existence of maximum and minimum erosion rates within the range of f_c and NPSH-3%.

References

1 Chan, W. K. Visualisation et erosion de la cavitation dans une roue de pompe centrifuge. These Docteur-Ing., ENSAM, 1984
2 Deeprose, W. M. and Merry, H. Scaling for performance prediction. Stirling, 6–8 Sept. 1977, 123–130
3 Hammitt, F. G. *Cavitation and Multiphase Flow Phenomena.* McGraw-Hill, New York, 1981
4 Kato, H., Maeda, M., and Nakashima, Y. A comparison and evaluation of various cavitation erosion test methods. Cavitation Erosion in Fluid Systems Symp. Boulder, Colorado